Available online at www.sciencedirect.com
ScienceDirect
Journal of Organometallic Chemistry 692 (2007) 3019–3026
Journal of Organometallic Chemistry
www.elsevier.com/locate/jorganchem

Synthesis, characterization, antibacterial and cytotoxic activity of new palladium(II) complexes with dithiocarbamate ligands: X-ray structure of bis(dibenzyl-1-S:S′-dithiocarbamato)Pd(II)

Farkhanda Shaheen [a], Amin Badshah [a], Marcel Gielen [b,*], Michal Dusek [c], Karla Fejfarova [c], Dick de Vos [d], Bushra Mirza [e]

[a] *Department of Chemistry, Quaid-I-Azam University, Islamabad 45320, Pakistan*
[b] *Vrije Universiteit Brussel, Faculty of Engineering, HNMR Unit, B-1050 Brussels, Belgium*
[c] *Institute of Physics, Na Slovance, 182 21 Praha 8, Czech Republic*
[d] *Pharmachemie BV, P.O. Box 552, 2003 RN Haarlem, The Netherlands*
[e] *Department of Biology, Faculty of Biological Science, Quaid-I-Azam University, Islamabad 45320, Pakistan*

Received 23 January 2007; received in revised form 15 March 2007; accepted 15 March 2007
Available online 21 March 2007

Abstract

Six palladium(II) dithiocarbamates of general formula $Pd(AmDTC)_2$, where HAmDTC = aminedithiocarbamic acid, [Pd(II) piperidinedithiocarbamate (**1**), Pd(II) 4-methylpiperidinedithiocarbamate (**2**), Pd(II) *N*-methylbenzyldithiocarbamate (**3**), Pd(II) dibenzyldithiocarbamate (**4**), Pd(II) dicyclohexyldithiocarbamate (**5**), Pd(II) *N*-cyclohexyl-*N*-methyldithiocarbamate (**6**)] have been synthesized and characterized by elemental analyses, FT-IR, ^1H and ^{13}C NMR. The X-ray structure of Pd(II), compounds **3** and **4**, showed that the ligands are chelated by both sulfur atoms with bond angles S1–Pd–S4 = 179.24(2)° and S2–Pd–S3 = 179.09(5)°, with a distorted square planar geometry around Pd. All these complexes were screened for cytotoxic and antibacterial effects and showed significant antibacterial activity and no substantial in vitro cytotoxicity indicating specificity of the compounds.

Keywords: Dithiocarbamate; Palladium; Anti-bacterial activity; Cytotoxicity

1. Introduction

Dithiocarbamates are known to display both mono and bi-dentate co-ordination to transition metal centers. Transition metal complexes of dithiocarbamates present a wide range of applications in agriculture, medicine, industry, in analytical and organic chemistry [1–4], as fungicides, pesticides [5]. They were also used as molecular precursors in CVD processes [6]. Recently, palladium(II) complexes have attracted significant attention due to their biological [7] as well as catalytic applications [8], and also play a role in metallocyclation [9] due to strong bonds with dithiocarbamate, which prevent or at least limit the reactions with other sulfur-containing renal proteins [10]. Dithiocarbamate/dithioester complexes of Pt^{2+} and Pd^{2+} are known to exhibit antitumor properties [11,12] and cytotoxic activities against some tumor cells, such as lung, ovarian [13], melanoma, colon, renal, prostate and breast cancer [14]. Complexes of dithiocarbamate also exhibited antitumor activities against *pam.ras* cells [15]. Among them, the dithiocarbamate complexes $[M(S_2CNEt_2)(L)]NO_3$ (M = Pd, Pt; L = 2,2′-bipyridyl or 1,10-phenanthroline) showed antitumor activities against leukaemic cells [16]. Many Pd^{2+}/Pt^{2+} complexes with dithioesters and dithiocarbamates exhibit in vitro cytostatic activities against KB tumor cells [17,18]. Furthermore the diethylthiocarbamato complexes

* Corresponding author. Tel.: +32 2 629 32 79; fax: +32 2 629 32 81.
E-mail addresses: fshaheenpk@yahoo.com (F. Shaheen), mgielen@vub.ac.be (M. Gielen).

0022-328X/$ - see front matter © 2007 Elsevier B.V. All rights reserved.
doi:10.1016/j.jorganchem.2007.03.019

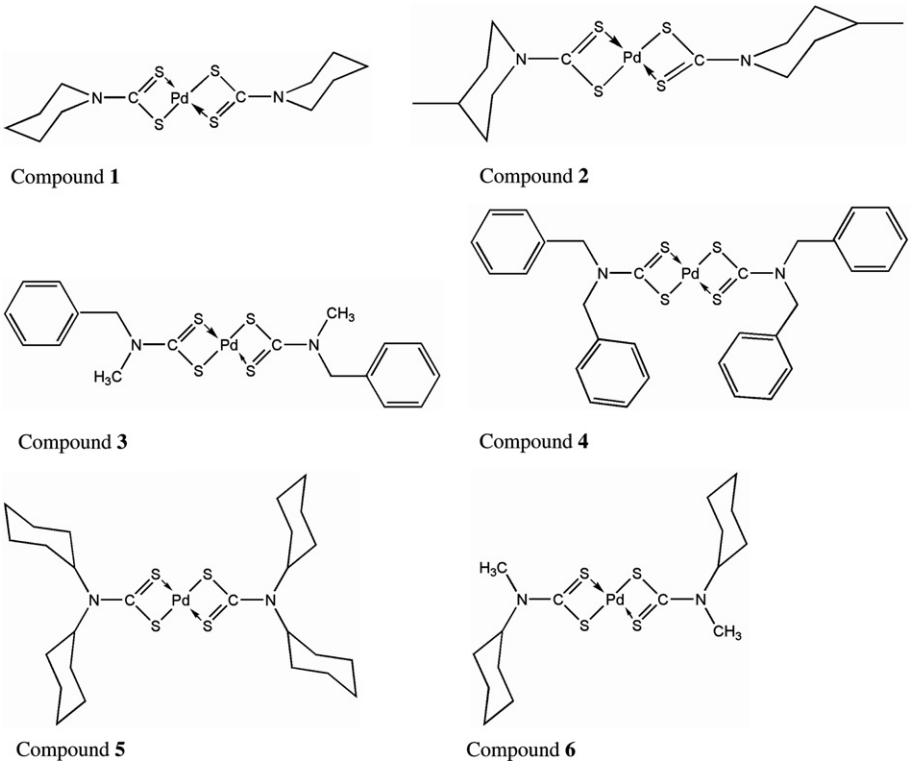

Scheme 1. Structures of compounds **1**–**6**.

of Pt^{2+} and Pd^{2+} exhibiting high anticancer activity together with a reduced toxicity, with respect to cisplatin and analogous compounds [19]. Recently we have reported the crystal structure of analogous complexes, bis(piperidine-1-dithiocarbamato)Pd(II), bis(4-methylpiperidine-1-S:S′-dithiocarbamato)Pd(II) and chloro[(4-methylpiperidine-1-S:S′-dithiocarbamato)(PPh_3)]Pd(II) [20,21].

In this paper, we report the synthesis and characterization of six palladium(II) aminedithiocarbamates of general formula $Pd(AmDTC)_2$, where H(AmDTC) = aminedithiocarbamic acid: [Pd(II) piperidinedithiocarbamate (**1**), Pd(II) 4-methylpiperidinedithiocarbamate (**2**), Pd(II) *N*-methylbenzyldithiocarbamate (**3**), Pd(II) dibenzyldithiocarbamate (**4**), Pd(II) dicyclohexyldithiocarbamate (**5**), Pd(II) *N*-cyclohexyl-*N*-methyldithiocarbamate (**6**) (see Scheme 1).

2. Experimental

2.1. Materials and methods

$PdCl_2$, substituted amines and all solvents, dichloromethane, diethyl ether, *n*-hexane, methanol were purchased from E-Merck, Germany and Aldrich. The compounds were characterized by elemental analyses, FT-IR, single crystal X-ray diffraction, ^1H and ^{13}C NMR spectroscopy. FT-IR spectra were recorded on a Perkin–Elmer FTIR 1000 spectrophotometer using KBr pellets in the 4000–400 cm^{-1} range, NMR measurements were carried out on a Bruker ARX 250 FT NMR spectrophotometer at 297 K in $CDCl_3$. The ^{13}C NMR spectra were obtained at a frequency of 300 MHz with ^1H broad band decoupling and are given relative to TMS.

2.2. Synthesis of substituted dithiocarbamic acids

Substituted dithiocarbamates were synthesized according to the literature method [22]. Typically, to a 4.0 ml solution of amines in methanol at 0 °C, carbon disulfide was added drop wise in a 1:1 molar ratio with constant stirring during 1 h. The solid product thus obtained was washed with an excess of methanol and dried in open air. It was re-crystallized from dichloromethane/*n*-hexane.

2.3. Synthesis of the complexes

To a suspension of $PdCl_2$ in dichloromethane (15 cm^3), a stoichiometric amount of substituted dithiocarbamic acids in dichloromethane (15 cm^3) was slowly added in a 1:2 metal:ligand molar ratio. The mixture was refluxed for 2 h with constant stirring. The clear solution then obtained was evaporated under reduced pressure 50–30%. Crystalline products were obtained after a slow evaporation of the solvent at room temperature. The general chemical reaction is shown by the following equation:

$$PdX_2 + 2H(AmDTC) \xrightarrow{MeOH} Pd(AmDTC)_2 + 2HX$$

All these crystalline solids are soluble in dichloromethane and chloroform. The elemental analyses of the complexes are given in Table 1.

Table 1
Elemental analysis of the $[Pd^{II}(Am^{a}DTC)_2]$ complexes

Complexes $[Pd^{II}(AmDTC)_2]$	Elemental analysis (%), observed (calculated)				M.p. (°C)	Molecular formula weight
	C	H	N	S		
$[Pd^{II}(pipDTC)_2]$ (**1**)	39.0 (39.4)	5.3 (5.4)	7.6 (7.5)	35.1 (35.0)	328–330(dec.)	365.31
$[Pd^{II}(MpipDTC)_2]$ (**2**)	35.9 (36.5)	5.2 (5.2)	6.0 (6.1)	27.8 (27.8)	260–261(dec.)	459.31
$[Pd^{II}(MBzDTC)_2]$ (**3**)	43.3 (43.2)	4.1 (4.0)	5.5 (5.6)	25.5 (25.6)	145–147	499.00
$[Pd^{II}(DBzDTC)_2]$ (**4**)	69.9 (71.0)	5.4 (5.5)	5.2 (5.5)	25.4 (25.2)	301–302(dec.)	507.00
$[Pd^{II}(DCyDTC)_2]$ (**5**)	52.3 (52.4)	7.5 (7.4)	4.5 (4.7)	21.7 (21.5)	300–302	595.00
$[Pd^{II}(CyMDTC)_2]$ (**6**)	39.5 (39.7)	5.5 (5.7)	5.5 (5.7)	26.6 (26.5)	287–289	483.00

[a] Am = piperidine, 4-methylpiperidine, dibenzylamine, *N*-methylbenzylamine, dicyclohexylamine, *N*-methylcyclohexylamine.

2.4. X-ray data collection and structure determination of complexes 3 and 4

Orange X-ray quality crystal of complex-3 was selected with a dimension $0.25 \times 0.10 \times 0.08$ mm and mounted on a Philips PW 1100 diffractometer (Mo Kα; $\lambda = 0.71073$ Å). Reflection data were collected by using limits $-7 \leqslant h \leqslant 5$, $-9 \leqslant k \leqslant 4$, $-12 \leqslant l \leqslant 12$, out of 1830 reflections 1698 were considered observed with $[I > 2\sigma(I)]$. Empirical absorption correction was applied using the local program based on Walker and Stuart [23]. The structure was solved by direct methods (SIR-97) [24] and refined with full-matrix least-squares (SHELXL-97) [25], using the wingx software package [26]. The program ORTEP for window was also used. Cell dimension were obtained by least-squares refinement of the setting angles of 25 accurately centered reflections: 1830 independent reflection (to $\theta \leqslant 25°$) were measure using by θ–2θ scans, background scans being taken on each side of the peak ($R_{int} = 0.000$). Atomic scattering factors were taken from International Tables for X-ray Crystallography (1974).

An yellow crystal of complex **4** ca. $0.259 \times 0.138 \times 0.061$ mm was mounted on Oxford Diffraction CCD-calibur2/Sapphire2 [27], at angle 2.5°, Mo Kα radiation filtered by graphite crystal monochromator, using diffraction detector mean area of resolution 8.3438, cell dimensions and their standard deviations derived by rotation method data acquisition using ω–2θ scans, densities of 28 577 reflections ($\theta < 26.71°$) measured by ω–2θ scans and background counts taken on each side of the peak, intensities of three standard reflection measured 9000 s showed no significant change during data collection. Integration of the CCD images was done by program CrysAlis RED (Oxford index diffraction 2004) [28]. The same program was used for indexing of the crystal shape, its refinement and absorption correction. Reflection data were collected by using limits $-17 < h > 14$, $-17 < k > 17$, $-20 < l > 20$, out of 11 397 reflections 8044 were considered observed with $I > 3\sigma(I)$. All calculations were carried out by using CrysAlis RED (for cell refinement, data reduction). SIR-2002 was used to solve the structure [29]. The structure was refined by using Jana 2000 [30], refinement of non-H atoms was done anisotropically and H atoms isotropically reduced R to a final value of 0.0354, $R_w = 0.0522$, weighting scheme based on counting statistics $w = 1/(\sigma^2(I) + 0.0009I^2)$, C–H distances were constrained at 0.96 Å to their ideal position, their isotropic displacement parameter were kept as 1.2 multiple of equivalent displacement parameter of the atoms to which the hydrogen is bonded. A final differences map showed no significant features.

2.5. Biological assays

2.5.1. Antibacterial assay

The antibacterial activity of all synthesized metal complexes has been investigated against six strains of bacteria (*Escherichia coli*, *Bacillus subtilis*, *Shigella flexenari*, *Staphylococcus aureus*, *Salmonella typhi*, and *Pseudomonas aeruginosa*) by the agar well diffusion method [31,32]. Imipenum was used as standard antibiotic. Three milligrams of the complexes were dissolved in 1 ml of DMSO. Centrifuged pellets of bacteria from a 24-h-old culture containing approximately 10^4–10^6 colony forming unit (CFU) per ml was spread on the surface of Muller Hinton Agar (MHA) plates. Wells were created in medium with the help of a sterile metallic borer and nutrients agar medium were prepared by suspending nutrient agar (Merck) 20 g in one liter of distilled water (pH 7.0), autoclaved and cooled down to 45 °C. Then it was seeded with 10 ml of prepared inocula to have 10^6 CFU/ml. Peter plates were prepared by pouring 75 ml of seeded nutrients agar. Experimental plates were incubated for 24 h and zones of inhibition (%) were measured and compared with standard antibiotic imipenum with zone inhibition of 20 and 22 mm, respectively [33,34]. The results are shown in Table 6.

2.5.2. Cytotoxicity screenings

The test and reference compounds were dissolved to a concentration of 250 000 ng/ml in full medium, by 20-fold dilution of a stock solution which contained 1 mg compound/200 µl. The compounds were taken into dimethylsulfoxide. Cytotoxicity was estimated by the microculture sulforhodamine B (SRB) test [34]. The human cancer cell lines examined in the present study were: A498, renal cancer; MCF-7, estrogen receptor (ER)+/progesterone receptor (PgR) + breast cancer; EVSA-T, estrogen receptor (ER)-/progesterone receptor (PgR)-breast cancer, H226,

non-small cell lung cancer; IGROV, ovarian cancer; M19 MEL, melanoma; and WIDR, colon cancer.

The experiment was started on day 0. On day 0, 10 000 cells per well were seeded into 96-wells flatbottom microtiter plates (falcon 3072, DB). The plates were incubated overnight at 37 °C, 5% CO_2 to allow the cells to adhere to the bottom. On day 1, a threefold dilution sequence of 10 steps was made in full medium, starting with the 250,000 ng/ml stock solution. Every dilution was used in quadruplicate by adding 200 μl to a column of four wells. This procedure results in a highest concentration of 625,000 ng/ml present in column 12. Column 2 was used for the blank. After incubation of 3 days, the plates were washed with PBS twice. Fluorescein diacetate (FDA) stock solution was diluted to 2 μg/ml with PBS and 200 μl of this solution was added to each of the control, experimental and blank wells. The plates were incubated for 30 min at 37 °C and the fluorescence generated from each well was measured at an excitation wavelength of 485 nm and an emission wavelength of 535 nm using an automated microplate reader (Labsystems Multiskan MS). Data were used for construction of concentration–response curves and determination of the ID_{50} value by use of Deltasoft 3 software. The variability of the in vitro cytotoxicity test depends on inter alia the cell lines used and the serum applied. With the same batch of cell lines and the same batch of serum the inter-experimental CV (coefficient of variation) is 1–11% depending on the cell line and the intra-experimental CV is 2–4%. These values may be higher with other batches of cell lines and/or serum. For details on the in vitro cytotoxicity tests, see Refs. [34,35].

3. Result and discussion

3.1. Infrared spectroscopy

The most significant bands recorded in the IR spectra of all synthesized complexes are listed in Table 2. Tentative assignments are made according to the literature [36]. The absence of ν(S–H) vibrations (which were observed in the parent dithiocarbamates in the range of 2754–2654 cm^{-1}), in the synthesized complexes indicate that the S–H proton is replaced by a metal ion, and the C–N and C–S stretching frequencies that can be used to differentiate between mono- and bidentate modes of binding of dithiocarbamate ligands [37]. The position of the ν(C–N) absorption is at 1438–1410 cm^{-1} in the free ligands and complexes. The 1500–1470 cm^{-1} region allows to identify the nature of the resulting complexes [38]: in the complexes showing an S–S chelate to metal coordination, the ν(C–N) stretching frequencies are shifted to higher frequency by about ~50 cm^{-1} on coordination with palladium. The energy of the dithiocarbamate ν(C–N) band is intermediate between the stretching frequencies associated with singly and doubly bonded carbon and nitrogen, and the double bond character is increased by electron delocalization towards the metal center [39]. In the case of a singular coordination with the thiocarbonyl sulfur, the shift is only approximately 10–20 cm^{-1} [40]. This suggests that the C–N bonds in the complexes have some partial double bond character. Partial double bond character for the C–N bond would result in some partial double bond character for the C–S bonds [41,42]. This band also defines a carbon-nitrogen bond order intermediate between a single bond-characteristic frequency (1350–1250 cm^{-1}) and a double bond (1680–1470 cm^{-1}) [43]. The presence of only one band in the region 1061–940 cm^{-1} is assumed to indicate a completely symmetrically bonding of the dithiocarbamate ligand, acting in a bidentate fashion, while a split band indicative of an unsymmetrically bound bidentate ligand [38,44] (see Table 2).

In the complexes reported in this paper, the presence of only one band in the region of 1061–940 cm^{-1}, the ν(CSS) mode, suggests a symmetrical behavior of the bidentate dithiocarbamate moiety. According to the literature [37,41,45] for complexes, the $\Delta\nu$ values $\nu(CSS)_{asym} - \nu(CSS)_{sym}$ are 120–137 cm^{-1}, indicating that the sulfur atoms of the dithiocarbamate group are linked to the central tin in a bidentate fashion. A new M-S band appeared in the region 400–300 cm^{-1} in the complexes due to (Pd–S) stretching [46] (see Table 2).

Table 2
Principal IR spectral data (cm^{-1})[a] of $[Pd^{II}(Am^{*}DTC)_2]$ complexes by using KBr pellets

Complexes $[Pd^{II}(AmDTC)_2]$	IR (ν, cm^{-1})			
	(C–S)	(Pd–S)	(C–N)	(C=S)
$[Pd^{II}(pipDTC)_2]$ (**1**)	1530 br	388 m	1485 s	1030 m
$[Pd^{II}(MpipDTC)_2]$ (**2**)	1529 m	392 m	1478 s	1034 m
$[Pd^{II}(MBzDTC)_2]$ (**3**)	1535 m	390 w	1470 s	995 w
$[Pd^{II}(DBzDTC)_2]$ (**4**)	1534 br	399 w	1461 s	1020 w
$[Pd^{II}(DCyDTC)_2]$ (**5**)	1545 m	335 m	1467 s	1032 m
$[Pd^{II}(CyMDTC)_2]$ (**6**)	1532 m	338 m	1458 s	1012 m

[a] s = strong, m = medium, w = weak, br = broad.

3.2. X-ray structure

In compound **3** (see Table 3) the palladium(II) ion is bonded to four sulfur atoms belonging to the two dithiocarbamate ligands. The palladium metal is an inversion centre of a square planar structure. The corresponding S1–Pd–S2 angles are 180°, 94.98° and 85.02°, respectively. The crystal is twinned and this probably affected some geometric parameters such as the C–S bond distances of the dithiocarbamate fragments (~2 Å). The bond distances of Pd–S are not equal and lie in the range 2.299(3)–2.312(3) Å (see Fig. 1) (see Table 5).

The molecular structure of the compound **4** (see Table 4) is depicted in Fig. 2. The geometry around the Pd(II) center is a slightly distorted square plane. The corresponding bond angles S(1)–Pd(1)–S(4) and S(2)–Pd(1)–S(3) are equal to 179.24(2)° and 179.095°, respectively, The metal–ligand bond distances are Pd(1)–S(1) = 2.3290(6) Å and Pd(1)–S(2) = 2.3385 Å.

Table 3
Crystal data and structure refinement for compound **3**

Empirical formula	$C_{18}H_{20}N_2PdS_4$
Formula weight	499.00
Temperature (K)	293(2)
Wavelength (Å)	0.71073
Crystal system	Triclinic
Space group	$P\bar{1}$
Unit cell dimensions	
a (Å)	6.526(5)
b (Å)	8.155(7)
c (Å)	10.567(7)
α (°)	89.55(7)
β (°)	78.50(7)
γ (°)	71.44(6)
V (Å^3)	521.5(7)
Z	1
D_{calc} (Mg/m^3)	1.589
Absorption coefficient (mm^{-1})	1.294
F(000)	252
Crystal size (mm)	$0.25 \times 0.10 \times 0.08$
θ Range for data collection (°)	3.20–25.00
Limiting indices	$-7 \leqslant h \leqslant 5$, $-9 \leqslant k \leqslant 4$, $-12 \leqslant l \leqslant 12$
Reflections collected/unique (R_{int})	1830/1830 (0.0000)
Completeness to $\theta = 25.00°$ (%)	99.5
Absorption correction	Empirical
Maximum and minimum transmission	1.000 and 0.861
Refinement method	Full-matrix least-squares on F^2
Data/restraints/parameters	1830/0/116
Goodness-of-fit on F^2	1.074
Final R indices [$I > 2\sigma(I)$]	$R_1 = 0.0561$, $wR_2 = 0.1386$
R indices (all data)	$R_1 = 0.0605$, $wR_2 = 0.1426$
Largest difference in peak and hole (e Å^{-3})	1.070 and −0.975

Table 4
Crystal data and structure refinement for compound **4**

Empirical formula	$C_{30}H_{28}N_2PdS_4$
Formula weight	651.2
Temperature (K)	293(2)
Wavelength (Å)	0.71073
Crystal system, space group	Triclinic, $P\bar{1}$
Unit cell dimensions	
a Å	13.8787(10)
b Å	14.3656(10)
c Å	16.4788(10)
α (°)	64.337(6)
β (°)	72.330(6)
γ (°)	83.290(6)
V (Å^3)	2821.3(4)
Z	4
D_{calc} (Mg/m^3)	1.5327
Absorption coefficient (mm^{-1})	0.977
F(000)	1328
Crystal size (mm)	$0.25 \times 0.13 \times 0.06$
θ Range for data collection (°)	2.48–26.49
Limiting indices	$-17 \leqslant h \leqslant 14$, $-17 \leqslant k \leqslant 17$, $-20 \leqslant l \leqslant 20$
Reflections collected/unique (R_{int})	28577/11397 (0.0190)
Completeness to $\theta = 26.71$ (%)	99.5
Absorption correction	Analytical
Maximum and minimum transmission	0.812 and 0.689
Refinement method	Full-matrix least-squares on F^2
Data/restraints/parameters	28577/0/667
Goodness-of-fit on F^2	0.94
Final R indices [$I > 3\sigma(I)$]	$R_1 = 0.0206$, $wR_2 = 0.0498$
R indices (all data)	$R_1 = 0.0354$, $wR_2 = 0.0522$
Largest difference in peak and hole (eÅ^{-3})	0.21 and −0.15

3.3. NMR study

Generally, the absence of S–H protons and a slight downfield shift of the protons in the NMR spectra of all complexes were observed, which indicates that the ligands are coordinated to palladium through sulfur atoms [47]. The mode of coordination has also been confirmed by single crystal X-ray diffraction. In the piperidinedithiocarbamate complex **1**, the methylene protons belonging to the $(CH_2)_3$ moiety exhibit downfield shifts in the range of 1.09–2.63 ppm and two signal appeared around 3.73–3.87 ppm for the NCH_2 methylene protons of $N(CH_2)_2$ originated from the different position (*syn* or *anti*) with respect to the thiocarbonyl group in the square planar molecule, the separation being larger than in the free dithiocarbamic acids due to coordination. The appearance of two signals is related to the barrier of rotation about the C–N bond [48], which makes the nitrogen substituents magnetically non-equivalent [49]. Similarly, for the 4-methylpiperidinedithiocarbamate complex **2**, peaks due to methyl and methylene protons were observed in the region 0.90–2.51 ppm, the methyl protons appearing as a doublet at 0.98 ppm ($\Delta\delta = 0.029$ ppm, $^3J_{HH} = 8.7$ Hz) and the N-$(CH_2)_2$ methylene protons being detected at 3.93 ppm and 4.64 ppm. In complex **3**, the N-CH_2 protons are

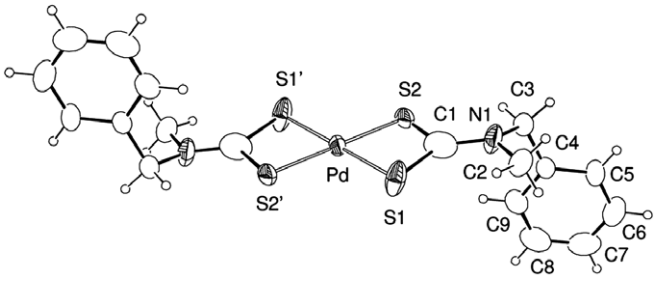

Fig. 1. ORTEP view of the palladium complex **3**.

non-equivalent and appear as two doublets at 4.75 ($\Delta\delta = 0.0230$ ppm, $^2J_{HH} = 6.9$ Hz) and at 5.21 ppm ($\Delta\delta = 0.0233$ ppm, $^2J_{HH} = 7$ Hz). One signal is present for the N-CH_3 proton at 3.17 ppm. A similar behavior for N-CH_2 is observed in the *N*,*N*′-dibenzyldithiocarbamate complex **4**. The proton spectrum of the *N*,*N*-dicyclohexyldithiocarbamate complex **5** is very simple:the CH protons bound to nitrogen show a complex pattern between 5.31 and 5.17 ppm and the signals of chain methylene protons were observed in the ranges 0.90–2.19. In the case of the *N*-cyclohexyl-*N*-methyldithiocarbamate complex **6**, a single resonance of methyl protons was observed as a singlet at 3.26 ppm and *N*-cyclohexyl protons

Table 5
Bond lengths (Å) and angles (°) for compound **3**

Bond lengths (Å)		Bond angles (°)	
C(1)–S(1)	1.816(11)	N(1)–C(1)–S(1)	124.5(7)
N(1)–C(1)	1.425(13)	N(1)–C(1)–S(2)	126.4(7)
C(1)–S(2)	2.007(12)	S(1)–C(1)–S(2)	109.1(6)
S(1)–Pd	2.299(3)	C(1)–S(1)–Pd	84.8(4)
S(2)–Pd	2.312(3)	C(1)–S(2)–Pd	80.4(3)
Pd–S(1)#1	2.299(3)	S(1)–Pd–S(1)#1	180.0
Pd–S(2)#1	2.312(3)	S(1)–Pd–S(2)	85.02(10)
		S(1)#1–Pd–S(2)	94.98(10)
		S(1)–Pd–S(2)#1	94.98(10)
		S(1)#1–Pd–S(2)#1	85.02(10)
		S(2)–Pd–S(2)#1	180.00(17)

Symmetry transformations used to generate equivalent atoms: #1 $-x$, $-y$, $-z$.

Table 6
Selected bond distances (Å) and bond angles (°) for compound **4**

Bond lengths (Å)		Bond angles (°)	
S(1)–Pd	2.299(3)	N(1)–C(1)–S(1)	124.5(7)
S(2)–Pd	2.312(3)	N(1)–C(1)–S(2)	126.4(7)
Pd–S(1)#1	2.299(3)	S(1)–C(1)–S(2)	109.1(6)
Pd–S(2)#1	2.312(3)	C(1)–S(1)–Pd	84.8(4)
		C(1)–S(2)–Pd	80.4(3)
		S(1)–Pd–S(1)#1	180.0
		S(1)–Pd–S(2)	85.02(10)
		S(1)#1–Pd–S(2)	94.98(10)
		S(1)–Pd–S(2)#1	94.98(10)
		S(1)#1–Pd–S(2)#1	85.02(10)
		S(2)–Pd–S(2)#1	180.00(17)

Symmetry transformations used to generate equivalent atoms: #1 $-x$, $-y$, $-z$.

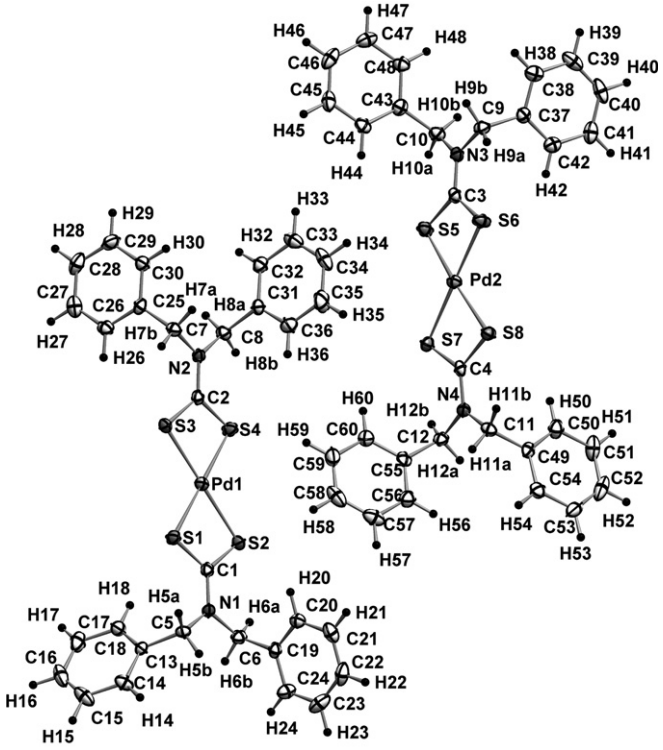

Fig. 2. Diamond view of the palladium complex **4**.

were observed between 0.90–2.9 and 4.00–5.00 ppm, respectively.

The $^{13}C\{^1H\}$ NMR spectra of all the complexes were recorded for $CDCl_3$ solutions. The resonance of the –CSS carbon was observed around 203 ppm, about 5–6 ppm downfield shift compared to the free dithiocarbamic acids. The downfield shift can be ascribed to the bidentate nature of the dithiocarbamates. Moreover, a significant downfield shift was observed for the C–N carbons. The downfield shift is consistent with an increase in the double bond character of C–N bond. The other resonances were only slightly shifted. ^{13}C NMR data of the compounds are given in Table 7.

Table 7
^{13}C NMR chemical shifts, δ (ppm) for the Pd^{II} complexes **1**–**6**

Compounds	C1	C2	C3	C4	C5	CH_3
$[Pd^{II}(pipDTC)_2]$ (**1**)	208.6	47.9	25.7	24.7	–	
$[Pd^{II}(MpipDTC)_2]$ (**2**)	206.4	47.3	31.3	27.4	–	23.4
$[Pd^{II}(MBzDTC)_2]$ (**3**)	206.5	59.9	142.7	132.0	129.7	29.7
$[Pd^{II}(DBzDTC)_2]$ (**4**)	209.3	58.9	141.0	129.8	127.7	–
$[Pd^{II}(DCyDTC)_2]$ (**5**)	203.3	63.0	32.7	26.2	25.7	–
$[Pd^{II}(CyMDTC)_2]$ (**6**)	206.5	58.6	29.7	25.2	29.0	30.7

3.4. Biological assays

3.4.1. Antibacterial inhibition studies

Metal–dithiocarbamates are capable of inhibiting bacterial growth and activity by interfering with the metabolic processes in the bacteria. In the present work, we have synthesized dithiocarbamate Pd(II) complexes. The antibacterial activity of the Pd(II) complexes have been determined against six strains of bacteria (*E. coli*, *B. subtilis*, *Shigella flexenari*, *Staphylococcus aureus*, *Samonella typhi*, and *P. aeruginosa*). The results are given in Table 8. Significant anti-bacterial activities were observed as compared to a standard drug except for complexes (**4**) and (**5**). The metal complexes containing piperidine (**1**), 4-methylpiperridine (**2**), *N*-methylbenzylamine (**3**) exhibit a good activity against *E. coli*. The metal complexes of dicyclohexyldithiocarbamate (**5**) and *N*-cyclohexyl-*N*-methyldithiocarbamate (**6**) exhibit a low activity against all reported bacteria, except "*Shigella flexenari*".

3.4.2. Cytotoxicity screenings

The results of the in vitro cytoxicity tests of compounds **1**–**6** are given in Table 1 as the inhibition doses ID_{50} observed against a panel of seven human tumour cell lines, MCF-7 and EVSA-T, two breast cancers, WiDr, a colon cancer, IGROV, an ovarian cancer, M19 MEL, a melanoma, A248, a renal cancer, and H226, a non-small cell lung cancer. The cytotoxicity results are compared with those obtained for clinically used reference compounds like doxorubicin DOX, cisplatin CPT, 5-fluorouracil 5FU, methotrexate MTX, etoposide ETO, and taxol TAX.

Table 8
Antibacterial Activity of the $[Pd^{II}(Am^{*}DTC)_2]$ complexes: zones of inhibition (in %)

Name of bacteria	% Zone of inhibition of samples (mm)						% Zone of inhibition of standard drug (mm)
	Cdp-1	Cdp-2	Cdp-3	Cdp-4	Cdp-5	Cdp-6	
Escherichia coli	28	27	22	20	18	24	33
Bacillus subtilis	18	12	14	23	20	20	30
Shigella flexenari	–	–	10	15	–	14	35
Staphylococcus aureus	21	25	23	19	29	20	43
Samonella typhi	23	18	27	14	23	33	25
Pseudomonas aeruginosa	31	18	16	19	22	18	40

Concentration of the standard drug (''Imipenum'') = 10 μg/disc.
Concentration of sample = 3 mg/ml.
–, No activity.

Table 9
Inhibition doses ID_{50}

Compound	A498	EVSA-T	H226	IGROV	M19MEL	MCF-7	WiDr
1	38688	46807	37535	38616	51168	38141	48690
2	37033	37992	37957	59428	49184	30168	43790
3	10084	2112	14616	1032	8818	10855	13780
DOX	90	8	199	60	16	10	11
CPT	2253	422	3269	169	558	699	967
5FU	143	475	340	297	442	750	225
MTX	37	5	2287	7	23	18	<3
ETO	1314	317	3934	580	505	2594	150
TAX	<3	<3	<3	<3	<3	<3	<3

It is evident from Table 9 that the studied compounds **1** and **2** exhibit very low cytotoxic activities whereas compound **3** shows mostly a low activity.

4. Conclusion

The complexes reported here have been obtained in the crystalline state, and the structures of two of them are reported. This study provides useful information about the bonding nature in the Pd(II) complexes, and the spectroscopic techniques used support and suggest that the coordination in all the $Pd^{II}(DTC)_2$ complexes yield a square planar geometry through the sulfur donating atoms, the NCSS group coordinating the metal center in a bidentate symmetrical mode. The in vitro antibacterial activities of the synthesized complexes have been studied by testing them in various bacterial strains which shows their inhibitory effect. It is important to observe that this antibacterial effect is not accompanied by cytotoxicity. This indicates a certain degree of specificity of the compounds studied.

Acknowledgements

The authors are thankful to Quaid-I-Azam University, Islamabad, Pakistan for financial support. The in vitro cytotoxicity experiments were carried out by Ms. P.F. van Cuijk in the Laboratory of Translational Pharmacology, Department of Medical Oncology, Erasmus Medical Center, Rotterdam, The Netherlands, under the supervision of Dr. E.A.C. Wiemer and Prof. Dr. G. Stoter.

Appendix A. Supplementary material

CCDC 296816 and 611518 contain the supplementary crystallographic data for **3** and **4**, respectively. These data can be obtained free of charge via http://www.ccdc.cam.ac.uk/conts/retrieving.html, or from the Cambridge Crystallographic Data Centre, 12 Union Road, Cambridge CB2 1EZ, UK; fax: (+44) 1223-336-033; or e-mail: deposit@ccdc.cam.ac.uk. Supplementary data associated with this article can be found, in the online version, at doi:10.1016/j.jorganchem.2007.03.019.

References

[1] R.J. Magee, J.O. Hill, Rev. Anal. Chem. 8 (1985) 5.
[2] A.M. Bond, R.L. Martin, Coord. Chem. Rev. 54 (1984) 23.
[3] A.L.J. Rao, N. Verma, A. Kumar, J. Kapoor, Chem. Environ. Res. 4 (1995) 163.
[4] E.M. Walker, H.F. Hardin, G.L. Gale, M.E. Reifsteck, D.J. Connon, M.M. Jones, Res. Common, Chem. Path. Pharmacol. 63 (1989) 101.
[5] D.J. Echobicon, in: D.J. Echobicon, R.M. Joy (Eds.), Pesticides and Neurological Diseases, second ed., CRC Press, Boca Raton, FL, 1994, p. 313.
[6] M. Bochmann, Chem. Vap. Deposition 2 (1996) 85.
[7] V. Alverdi, L. Giovagnini, C. Marzano, R. Seraglia, F. Bettio, S. Sitran, R. Graziani, D. Fregona, J. Inorg. Biochem. 98 (2004) 1117.
[8] J. Bravo, M.B. Cordero, J.S. Casas, M.V. Castano, A. Sanchez, J. Sordo, J. Organomet. Chem. 513 (1996) 63.
[9] B.E. Ali, K. Okuro, G. Vasapollo, H. Alper, J. Am. Chem. Soc. 118 (1996) 4264.
[10] D. Fregona, L. Giovagnini, L. Ronconi, C. Marzano, A. Trevisan, S. Sitran, B. Biondi, F. Bordin, J. Inorg. Biochem. 93 (2003) 181.
[11] R. Mital, N. Jain, T.S. Srivastava, Inorg. Chim. Acta 166 (1989) 135.

[12] G. Faraglia, D. Fregona, S. Sitran, L. Giovagnini, C. Marzano, F. Baccichetti, U. Cesellato, J. Inorg. Biochem. 83 (2001) 31.
[13] P.I. O'Dwyer, J.P. Stevenson, S.W. Johnson, in: B. Lippert (Ed.), Cisplatin: Chemistry and Biochemistry of a Leading Anticancer Drug, Wiley–VCH, Weinheim, 1999, pp. 31–69.
[14] A. Scozzafava, A. Mastrolorenzo, T.C. Supuran, Bioorg. Med. Chem. Lett. 10 (2000) 1887.
[15] A.I. Maztesanz, J.M. Perez, P. Navarro, J.M. Moreno, E. Colacio, P. Souza, J. Inorg. Biochem. 76 (1999) 29.
[16] G. Faraglia, L. Sindellari, V. Cerehi, A. Furlani, A. Papioannou, V. Scarcia, Transition Met. Chem. 18 (1993) 45.
[17] A. Furlani, V. Scarcia, G. Faraglia, L. Sindellari, L. Trincia, M. Nicolini, Eur. J. Med. Chem. 21 (1986) 261.
[18] G. Faraglia, L. Sindellari, S. Sitran, Thermochim. Acta 161 (1990) 63.
[19] K. Lemma, S.K.C. Elmroth, L.I. Elding, J. Chem. Soc., Dalton. Trans. (2002) 1281.
[20] F. Shaheen, A. Badshah, S. Anjum, S. Ali, Acta. Crystallgr., Sect. E 62 (2006) m329;
S. Shahzadi, S. Ali, A. Badshah, F. Shaheen, F. Ahmad, M. Fettouhi, J. Chem. Crystallogr. 36 (2006) 567.
[21] F. Shaheen, M.N. Haq, A. Badshah, K. Wurst, S. Ali, Acta Crystallogr., Sect. E 62 (2006) m138.
[22] A.I. Vogel, A Textbook of Practical Organic Chemistry, ELBS Publication, London, 1968, p. 499.
[23] N. Walker, D. Stuart, Acta Cryst. A 39 (1983) 158.
[24] A. Altomare, C.M. Burla, M. Camalli, G. Cascarano, C. Giacovazzo, A. Guagliardi, G.G.A. Moliterni, G. Polidori, R. Spagna SIR-97: the program, J. Appl. Crystallogr. 32 (1999) 115.
[25] G.M. Sheldrick, SHELXL-97, University of Göttingen, Göttingen, Germany, 1997.
[26] (a) M. Nardelli, J. Appl. Crystallogr. 28 (1995) 659;
(b) G. Polidori, R. Spagna, SIR-2002: the program, J. Appl. Crystallogr. 36 (2003) 1103.
[27] Oxford Diffraction, Crysalis CCD, CCD data collection, Oxford Diffraction Ltd., Oxford, UK, 2004.
[28] Oxford Diffraction, CrysAlis RED, CCD data reduction GUI, Oxford Diffraction Ltd., Oxford, UK, 2004.
[29] M.C. Burla, M. Camalli, B. Carrozzini, G. Cascarano, C. Giacovazzo, N. Walker, D. Stuart, Acta Crystallogr., Sect. A 39 (1983) 158.
[30] V. Petricek, M. Dusek, L. Palatinus, Jana (2000): Structure Determination Software Programs, Institute of Physics, Praha, Czech Republic, 2000.
[31] R. Carran, A. Maran, J.M. Montero, L. Fernadozlago, A. Dominguez, Plants Med. Phyto. 21 (1987) 195.
[32] S.U. Kazmi, S.N. Ali, S.A. Jamal, Atta-ur-Rehman, J. Pharm. Sci. 4 (1991) 113.
[33] S.S. Shaukat, N.A. Khan, F. Ahmad, Pak. J. Bot. 12 (1980) 97.
[34] Y.P. Keepers, P.E. Pizao, G.J. Peters, J. van Ark-Otte, B. Winograd, H.M. Pinedo, Eur. J. Cancer 27 (1991) 897.
[35] M.R. Boyd, Principle Practice Oncol. 3 (1989) 1.
[36] D. Fregona, L. Giovagnini, L. Ronconi, C. Marzano, A. Treeevisan, S. Sitran, B. Bordin, J. Inorg. Biochem. 93 (2003) 181.
[37] C.V.R. de Moura, A.P.G. De Sousa, R.M. Silva, A. Abras, M. Horner, A.J. Bortoluzzi, C.A.L. Filgueiras, J.L. Wardell, Polyhedron 18 (1999) 2961.
[38] G. Faraglia, S. Sitran, D. Montagner, Inorg. Chim. Acta 358 (2005) 971.
[39] S. Thirumaran, K. Ramalingam, Transition Met. Chem. 25 (2000) 60.
[40] D. Fregona, S. Tenconi, G. Faragila, S. Sitran, Polyhedron 16 (1997) 3795.
[41] H.D. Yin, C.H. Wang, C.L. Ma, Y. Wang, R.F. Zhang, Chin. J. Inorg. Chem. 18 (2002) 347.
[42] H.D. Yin, C.H. Wang, C.L. Ma, Y. Wang, R.F. Zhang, Chin. J. Org. Chem. 22 (2002) 183.
[43] J.J. Criado, J.A. Leopez Aria, B. Marcias, L.R. Fernandez Lago, Inorg. Chim. Acta 193 (1992) 229.
[44] L. Ronconi, C. Maccata, D. Barreca, R. Saini, M. Zancato, D. Fregona, Polyhedron 24 (2005) 521.
[45] E.R.T. Tiekink, V.J. Hall, M.A. Buntine, Z. Kristallogr. 214 (1999) 124.
[46] R.V. Parish, B.P. Howe, J.P. Wright, J. Mack, R.C. Pritchard, R.G. Buckley, A.M. Elsome, S.P. Fricker, Inorg. Chem. 35 (1996) 1659.
[47] G. Faraglia, S. Sitran, Inorg. Chim. Acta 176 (1990) 67.
[48] (a) A.E. Lemire, J.C. Thompson, Can. J. Chem. 48 (1970) 824;
(b) C.H. Yoder, A. Komoriya, J.E. Kochanowsky, F.H. Suydam, J. Am. Chem. Soc. 93 (1971) 6515.
[49] B.B. Kaul, K.B. Pandeya, J. Inorg. Nucl. Chem. 40 (1978) 171.